Physica E ▮ (▮▮▮▮) ▮▮▮–▮▮▮

Contents lists available at SciVerse ScienceDirect

Physica E

journal homepage: www.elsevier.com/locate/physe

Photoluminescence quenching and conductivity enhancement of PVK induced by CdS quantum dots

S. Masala [a], V. Bizzarro [b], M. Re [c], G. Nenna [a], F. Villani [a], C. Minarini [a], T. Di Luccio [a,*]

[a] ENEA Italian National Agency for New Technologies, Energy and Sustainable Economic Development, Centro Ricerche Portici, Piazzale E. Fermi 1, I-80055 Portici Naples, Italy
[b] IMAST Portici, Piazzale E. Fermi, I-80055 Portici Naples, Italy
[c] ENEA Italian National Agency for New Technologies, Energy and Sustainable Economic Development, Centro Ricerche Brindisi, SS7 Appia Km 713, I-72100 Brindisi, Italy

ARTICLE INFO

Article history:
Received 21 September 2011
Received in revised form
7 January 2012
Accepted 30 January 2012

ABSTRACT

In this work we studied the optical and transport properties of hybrid nanocomposites of CdS quantum dots (QDs) and poly(*N*-vinylcarbazole) (PVK) polymer. The CdS QDs were prepared by thermal decomposition (thermolysis) of a single source precursor, Cd bis-thiolate, in a high boiling solvent, octadecene (ODE). The optical characterization of the QDs has been carried out by UV–vis absorption and photoluminescence spectroscopy while the morphological properties have been investigated atomic force microscopy and transmission electron microscopy. The analyses have shown that CdS QDs of diameter below 6 nm can be synthesized by such route with good light emission in the UV range. The QDs have been dispersed in a poly(*N*-vinylcarbazole) (PVK) matrix to obtain a PVK:CdS nanocomposite layers. An increase of conductivity and a quenching of the photoluminescence have been observed when the nanocomposite layer was inserted in ITO/PVK:CdS/Al structures.

1. Introduction

The interest for semiconductor quantum dots (QDs) is still wide despite well consolidated results in the synthesis and study of their physical properties [1–3]. Because of the large surface/volume ratio and three-dimensional confinement of excitons they are among the top searched advanced materials in technological applications, e.g. sensors, organic light emitting devices (OLED) [4], solar cells [5] and biological markers [6]. Among the semiconductor materials the compounds belonging to the II–VI group have been extensively studied. In particular, CdS is a material with direct band gap of 2.41 eV [7] that exhibits a huge change in its optical properties as the size of the crystals is below 5 nm. The up-to-date most used synthesis methods of CdS QDs include inverse micelles [8], aqueous solution synthesis [9], organometallic synthesis [1,10] and thermolysis of suitable precursors such as metal thiolate molecules [11–13]. Concerning the synthesis in non-coordinating solvents a window of optimal reactants concentration and of reactants/ligand ratio has been systematically studied and a formidable control of the size and size distribution of CdS QDs with high quality optical properties has been recently reported [14].

In the current work we describe the synthesis of CdS QDs by means of thermolysis of Cd thiolate molecules in a non-coordinating solvent, octadecene (ODE). The thermolysis proceeds with the melting of the thiolate precursor (in the range 110–130 °C), and its transformation into the relative metal sulfide QDs at higher temperature (above 190 °C). The thermolysis has several advantages with respect to the other synthesis methods listed above. The first and most important aspect is that the synthesis involves a single source precursor. Consequently, there is no preparation complication due to multicomponents mixing, moreover no use of highly reactive reagents. In addition, it is a low cost and an environmental-friendly method. Concerning the metal thiolate precursors they are stable under room temperature and atmosphere conditions and are easy to prepare [15]. The mentioned properties are considered very promising for CdS QDs in applications involving polymeric nanocomposites for hybrid devices [4,5].

In previous works we used the thermolysis to synthesize CdS QDs in-situ within inert polymers, polystyrene and topas [12,13]. We found that the physical properties of the QDs depend on the annealing time and temperature ramp conditions. We have recently extended the same in-situ synthesis procedure to conjugated polymers to realize the active layer of hybrid solar cells [16] and OLEDs [17]. An alternative approach is the ex-situ preparation of the polymer/QD nanocomposite where the QDs can be embedded in the polymer matrix after the synthesis in solution. One advantage of the ex-situ method is the optimization of the chemical and physical properties of the QDs in view of their

* Corresponding author. Tel.: +39 081 7723244, fax: +39 081 7723344.
E-mail addresses: silvia.masala@enea.it (S. Masala), valentina.bizzarro@enea.it (V. Bizzarro), marilena.re@enea.it (M. Re), giuseppe.nenna@enea.it (G. Nenna), fulvia.villani@enea.it (F. Villani), carla.minarini@enea.it (C. Minarini), tiziana.diluccio@enea.it (T. Di Luccio).

1386-9477/$ - see front matter © 2012 Elsevier B.V. All rights reserved.
doi:10.1016/j.physe.2012.01.026

incorporation in the chosen polymer. In the present paper we describe the synthesis of CdS QDs by thermolysis in solution and their subsequent blend with the blue-emitting polymer poly(*N*-vinylcarbazole) (PVK). The as-prepared CdS QDs were fully characterized from the point of view of optical, structural, morphological and chemical properties by means of UV–vis absorption and photoluminescence (PL) spectroscopies, Atomic Force Microscopy (AFM), Transmission Electron Microscopy (TEM), Nuclear Magnetic Resonance (NMR) and Fourier Transform Infrared Spectroscopy (FT-IR). The QDs were then mixed with PVK to realize a diode structure ITO/PVK:CdS/Al. The optical and electrical properties of the nanocomposite device were studied and compared with those of a PVK analog structure. In presence of CdS QDs a photoluminescence quenching and a conductivity enhancement of PVK have been observed. The data are discussed in terms of band diagram levels.

2. Experimental section

CdS QD synthesis: The cadmium sulfide (CdS) QDs were synthesized by thermolysis of a cadmium bis-thiolate precursor in octadecene (ODE) (boiling temperature 315 °C). The cadmium-bis thiolate $Cd(SR)_2$ ($R=C_{12}H_{25}$) is formed by two S-terminating molecules bound to Cd atoms. It has been provided by ENEA Centro Ricerche Brindisi. The ODE was purchased by Alfa Aesar. The synthesis of the CdS QDs by thermolysis of $Cd(SR)_2$ was carried out by a simple one pot process. The concentration of the precursor in ODE was fixed at 3 mmol. Few milligrams of precursor were dispersed in ODE in a three necked round bottom flask equipped with a thermometer to measure the inner temperature of the solution, a Liebig condenser and an outer adapter to inject nitrogen vapors. The solution was heated by hot plate (FALC F 90 T) at an annealing temperature around 200 °C in two different ramps (Fig. 1). The reaction was stopped when the inner temperature reached the setup temperature by removing the flask from the hot plate and allowing the cool down in ambient condition. After the synthesis the CdS QDs were centrifuged (10,000 rpm), rinsed in hexane, collected and dried under vacuum.

PVK:CdS Nanocomposite preparation: The dried CdS QDs were redispersed in chlorobenzene and then mixed with a PVK chlorobenzene solution to prepare hybrid nanocomposites at a concentration PVK:CdS=25:1.

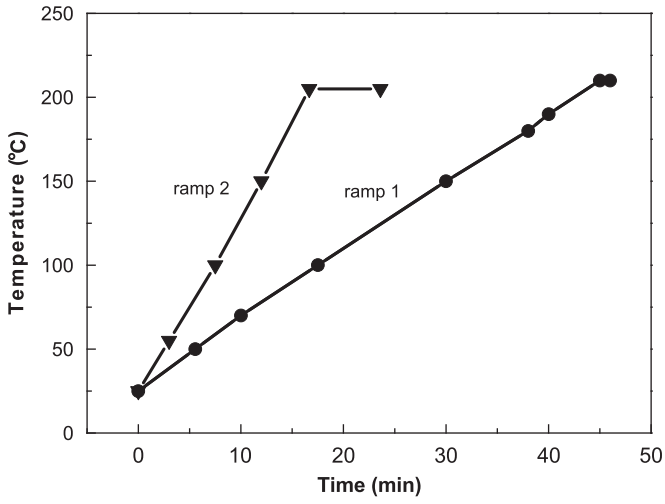

Fig. 1. Setup and inner temperature (T^{in}) used for the synthesis A and B (ramp 1) and C (ramp 2). The setup temperature for both ramps is plotted by solid lines, T^{in} is indicated by ● for sample A (B follows the same curve with final temperature of 190 °C) and ▼ for sample C, respectively.

Sample characterization: TEM analyses were allowed to determine the shape, the dimension and the structural phase of the CdS QDs. TEM experiments were performed by a Tecnai G2 F30 operating at 300 kV with spatial resolution of 0.205 nm, after dropping few microlitres of the solution on a carbon coated grid. The band gap and the size of the QDs were obtained by UV–vis absorption measurements using a Perkin Elmer Spectrophotometer Lambda 15. Photoluminescence (PL) spectroscopy was used to investigate the optical properties of the QDs in solution. The PL spectra were obtained by a Jasco FP-6200 spectrofluorimeter. Nuclear Magnetic Resonance (NMR) and Fourier Transform Infrared Spectroscopy (FT-IR) were used to investigate the chemical environment of the QDs surface. The NMR and solid state FT-IR spectra were recorded by a 400-MHz Bruker spectrometer and an IR Nicolet 5700 FTIR spectrometer, respectively. NMR and FT-IR results are reported in the Supplementary Data file. The morphology of the CdS QDs deposited on an MICA substrate was analyzed by Atomic Force Microspopy (AFM). The tapping mode measurements were carried out by Nanoscope IV Dimension DIGITAL INSTRUMENTS Veeco. A thin film of QDs was deposited by dispersing the CdS QDs in ethanol and sonicated at 50 °C for about 20 min then drop casted on a mica substrate previously cleaved. The substrate was kept at about 150 °C to avoid laminar flow and the aggregation process of the QDs as extensively discussed by Lee et al. [18].

The electrical properties of the hybrid nanocomposite were tested by inserting it in a diode structure ITO/PVK:CdS/Al. The PVK:CdS solution was deposited on patterned ITO/glass substrate by spinning the solution at 2000 rpm. The layer was 100 nm thick as estimated by an Alpha step IQ profiler. The top Al electrodes (150 nm thick) were evaporated through a shadow mask on top of PVK:CdS layer. The devices were characterized optically and electrically. In the first case we carried out photoluminescence measurements by a Fluorolog Horiba Jobin Yvon spectrofluorimeter equipped with a double monochromator. The electrical characteristics were measured using a Keithley 2400 semiconductor parameter analyzer in dark conditions.

3. Results and discussions

The transformation of $Cd(SR)_2$ into CdS QDs in the synthesis by thermolysis is due to decomposition of the precursor that first melts at about 120 °C then decomposes at 300 °C as indicated by thermogravimetric analysis (TGA) and differential scanning calorimetry (DSC). The thermolysis synthesis was carried out in two different procedures, namely ramp 1 and ramp 2 in Fig. 1 for a concentration of 3 mmol of precursor in ODE. In ramp 1 the setup temperature of the hot plate was raised gradually to 300 °C. The solution remained transparent and uncolored until the inner temperature T^{in} was 150 °C, then it changed color to yellowish. The reaction was stopped when T^{in} reached 210 °C by removing the flask from the hot plate. Two samples were prepared according to ramp 1, sample A and B at T^{in} equal to 210 and 190 °C, respectively. In ramp 2 (sample C) the setup temperature of the hot plate was fixed at 350 °C while T^{in} raised gradually to 210 °C. At this point T^{in} remained constant and the solution became yellowish. The reaction was stopped after 7 min. The ramp conditions for the three samples are listed in Table 1.

The UV–vis absorption spectra of the three samples A–C are shown in Fig. 2a. The measurements of both samples A and B show a weak absorption shoulder between 325 and 450 nm (3.0 and 3.5 eV, respectively) while the absorption curve relative to sample C shows a sharp excitonic peak located at 375 nm (3.32 eV). Such features occurring in the absorption spectra can be attributed to the lowest electronic transition occurring in CdS QDs

Table 1
Annealing conditions (temperature T^{in} and time), band gap and diameter values for solutions A–C as estimated by UV–vis absorption.

Sample	Ramp	T^{in} (°C)	Time (min)	Band gap (eV)	2R (nm)
A	1	210	46	2.80	6.04
B	1	190	40	2.80	6.04
C	2	210	23	3.08	4.61

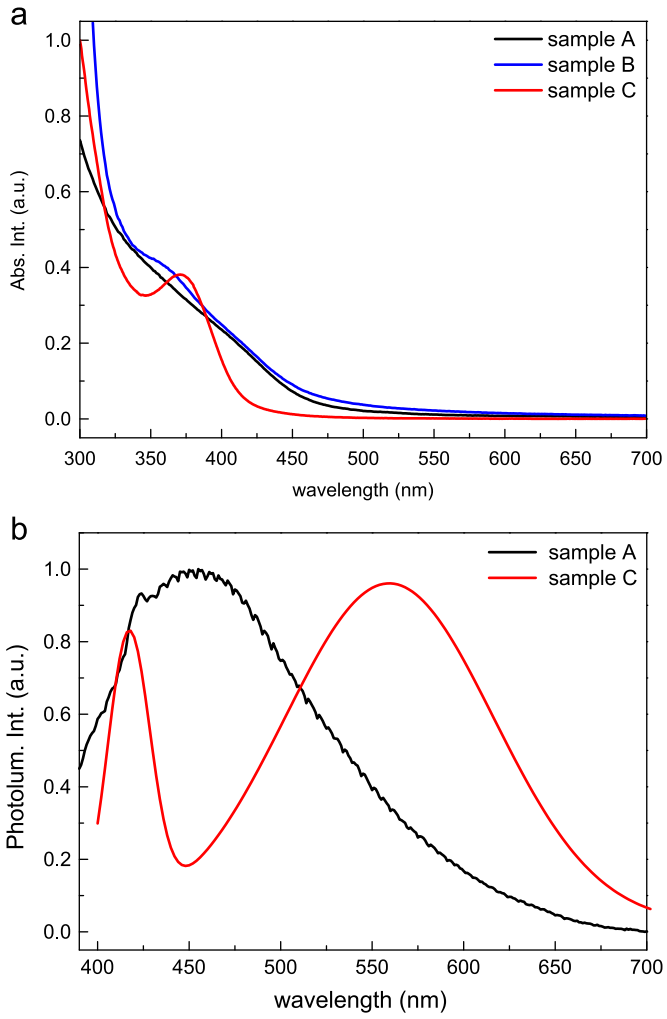

Fig. 2. (a) UV–vis absorption spectra of three solutions (A–C) after the synthesis of CdS QDs. The samples differ by the annealing process (Fig. 1). Sample C shows a well defined absorption peak due to charge carrier excitonic recombination typical of CdS QDs. (b) Photoluminescence spectra of the three excited at 375 nm. The excitonic emission is well defined only for sample C (peak at 420 nm) while the recombination in trap states is dominant in samples A and B.

[3,7]. The position of the absorption peak for sample C and the weak shoulders of samples A and B clearly demonstrate a blue shift compared to the bulk CdS (2.41 eV) [7] confirming the presence of QDs with size below the bulk exciton dimension of cadmium sulfide. We estimated the QDs size from the absorption data by calculating the energy gap and diameter of the QDs. The band gap has been evaluated by zero extrapolation of the straight line of $(\alpha h\nu)^2$ versus $h\nu$ plots. The band gap and diameter for the three samples are indicated in Table 1.

Concerning the photoluminescence (PL) properties, they are shown in Fig. 2b for all the solutions. The PL emission is quite different for samples A and B compared with sample C. Only in last sample the PL data show two distinct bands, a high energy band at 420 nm and a low energy band at 558 nm. The low energy peak is broad and stoke shifted and arises from deep trap emission. The high energy peak is a sharp peak located near the absorption edge (the stoke shift is about 40 meV) and can be attributed to luminescence by bound excitons [19]. Emission in trap states is due to surface defects such as sulfur vacancies. The data of Fig. 2b demonstrate that the quality of the defects is different for A and B synthesis than for C. In C the faster annealing process allows the formation of nearly monodisperse CdS QDs as shown from the very well defined absorption peak. On the contrary, a slow annealing as in the case of A and B produces QDs with a wide size distribution that broadens the absorption curve. This has consequences on the PL where the emission due to defects is blue-shifted and almost entirely covers the emission by direct recombination.

Local information about the size and shape of the QDs were obtained by TEM analyses. In the bright field image of Fig. 3a some QDs appear spherical while others show a needle shape. The average dimension evaluated from sampling 94 QDs is (5.9 $\pm$ 1.2) nm (see the histogram of the size distribution in Fig. 3b) which is slightly higher than that estimated by absorption measurements. From the high resolution HRTEM image in Fig. 3c it is possible to distinguish the lattice fringes of the QDs corresponding to a lattice distance of 0.31 nm. These fringes can be assigned to the (0 0 2) lattice planes of the wurtzite phase of CdS.

Further investigation of the morphology was achieved by AFM. The AFM images in Fig. 4 show the topography (a, b) and a cross section (c) of the QDs from sample C deposited on a mica substrate. The QDs have mostly circular shape over an investigated area of 1 μm × 1 μm. The mean surface roughness is 1.6 nm. The average dimension determined by statistical analysis ranges between 10 and 16 nm in lateral size with a standard deviation σ = 1.5 nm indicating that the QDs are almost uniformly synthesized and distributed on the MICA surface. However the QDs dimension is overestimated with respect to the diameter values calculated from the absorption spectrum (Table 1) and from TEM, due to both the slightly layered nature of the sample and the tip-curvature radius of about 8 nm [20]. Anyway, the AFM analysis demonstrate that the feasibility of realizing a layer of QDs on a flat substrate adopting a very easy method which avoids the QD aggregation.

The optical analyses have indicated that CdS QDs with a well defined absorption peak and a good photoluminescence signal can be synthesized at a temperature as low as 210 °C when the annealing process is relatively fast as in sample C. Such annealing temperature value was chosen to be high enough for the precursor to start the decomposition and the CdS nuclei to form. Higher temperatures and higher precursor concentration have been avoided since it has been proved that they produce larger QDs and aggregation that negatively affect the optical performances [13]. On the other hand, if the annealing temperature does not reach the decomposition temperature of the precursor, residuals of the thiol chains of the precursor are likely to be present as capping layer around the QDs. Therefore, further investigations were performed by NMR and FT-IR spectroscopy (reported in the Supplementary Data) in order to explore the surface and bulk properties of the CdS QDs. In particular we measured the sample C after the extraction by solution state and ^{1}H NMR and compared with the same measurement on the precursor. The spectra collected show three signals at 1–2 ppm due to aliphatic protons of organic chains and one broad signal in the same region attributable to protons of water molecule [21]. Concerning the organic chains FT-IR spectra also show a signal at 2400 cm^{-1} typical of the S–H groups of thiol molecules. This result together with ^{1}H NMR aliphatic signals and the QDs

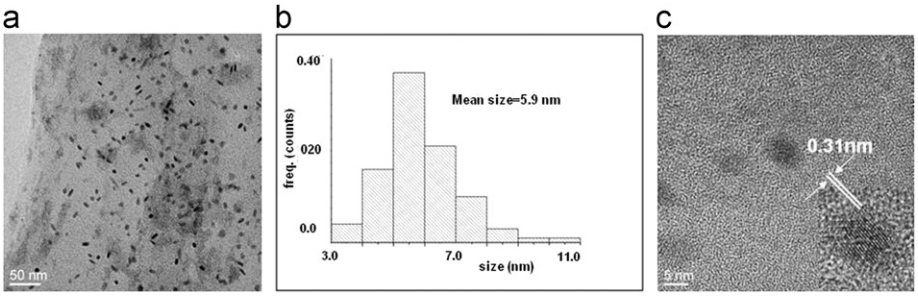

Fig. 3. TEM analyses of sample C: (a) bright field image; (b) histogram of the size distribution showing an average diameter of 5.9 nm; (c) HRTEM on some of the QDs of (a): lattice fringes can be seen with spacing of 0.31 nm.

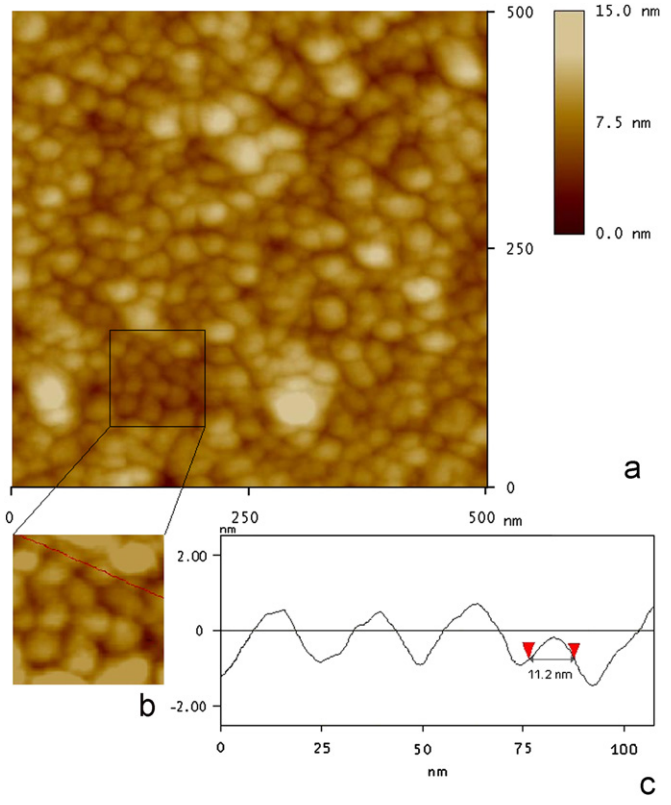

Fig. 4. (a) Tapping mode AFM image of CdS QDs (sample C); (b) blow up image (scan size 100 nm × 100 nm, height scale 5 nm) and (c) section analysis taken along the straight line.

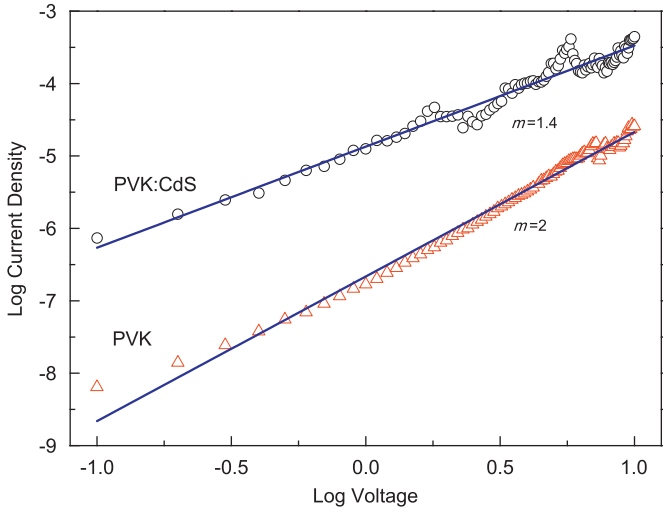

Fig. 5. Current–voltage (IV) characteristics in Log–Log scale of two devices: ITO/PVK/Al and ITO/PVK:CdS/Al. The data are well fitted with power law $J=V^m$.

characteristic of being completely and quickly dispersed in organic solvents, leads to the conclusion that parts of the thiol chains are bound to the surface of the QDs.

The presence of a capping layer surrounding the QDs is expected to influence the optical and electrical performances of nanocomposites of QDs and polymers. To study such influence PVK:CdS nanocomposite devices were prepared by blending QDs of sample C and PVK in PVK:CdS=25:1 w/w ratio. The nanocomposite was sandwiched between a patterned ITO/glass substrate and an Al top electrode. Fig. 5 shows the current density–voltage characteristics of the ITO/PVK:CdS/Al and ITO/PVK/Al reference devices. The CdS QDs in the PVK matrix produce an enhancement of the current density of about two orders of magnitude. Plotting the data in logarithmic scale, the exponent m of $J=V^m$ is immediately evaluated from a linear fit for both devices. The values found from the fit are $m=1.4$ for the ITO/PVK:CdS/Al device and $m=2$ for ITO/PVK/Al device. In the last case $m=2$ agrees with the expected value for the charge transport mechanism in conductive polymers as described by the SCLC (Space Charge Limited Current) model [22]. On the contrary, the value of $m=1.4$ in the ITO/PVK:CdS/Al indicates that the charge conduction mechanism is modified by the QDs from SCLC towards an ohmic behavior [23]. The conduction is due not only to holes injected from ITO to PVK but also to electrons injected from the cathode to CdS. The band diagram of the ITO/PVK:CdS/Al device structure is presented in Fig. 6. The values of the highest occupied molecular orbital (HOMO) and lowest unoccupied molecular orbital (LUMO) of PVK as well as the valence band (VB) of CdS have been taken from the literature [24], while the conduction band of CdS has been evaluated from the band gap measured by UV absorption data listed in Table 1. The close matching between the CB of CdS and the Fermi level of Al allows electrons to move easily from the cathode to the CdS QDs.

The volume fraction of the nanoparticles corresponding to the used concentration (4%) is $x=0.01$. At this concentration the calculated mean distance among the particles is about 22 nm. It is below the percolation threshold, as found by other groups on PVK:CdS [25], who also find an increase of mobility at very low nanoparticle concentration.

The optical properties of the nanocomposite were investigated by measuring the photoluminescence signal directly on the ITO/PVK:CdS/Al and ITO/PVK/Al devices, as shown in Fig. 7, using an excitation wavelength of 325 nm. The two peaks observed in PVK at 411 and 520 nm are due to excimers of the carbazole groups. These peaks remain in the same position when the QDs are dispersed in the PVK matrix but their intensity is greatly reduced. In addition the CdS PL signal observed at 420 nm in Fig. 1 is not detected here. The quenched signal in presence of CdS QDs

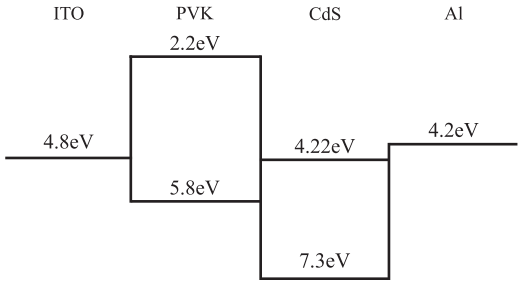

Fig. 6. Band diagram of the ITO/PVK:CdS/Al device.

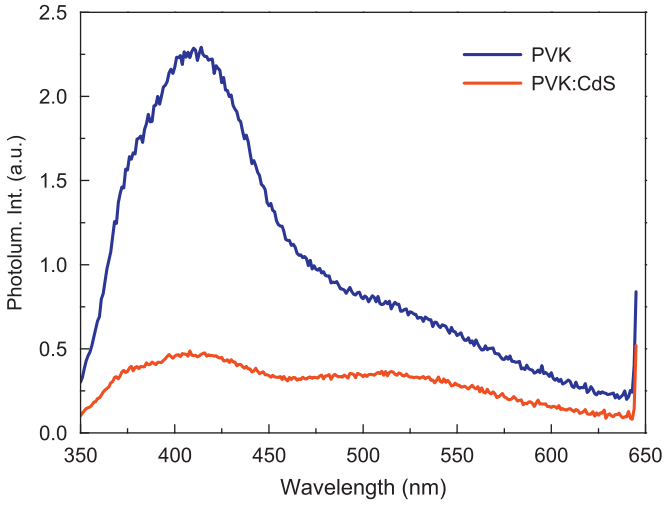

Fig. 7. Photoluminescence at 325 nm excitation wavelength of the nanocomposite device: ITO/PVK:CdS/Al and the reference device ITO/PVK/Al.

together with the absence of the band gap emission from CdS has been explained by other groups by interfacial charge transfer between the polymer and the QDs energy levels [24]. In presence of CdS a charge transfer of the excited electrons from the LUMO of PVK to the CB of CdS can compete with the radiative recombination with holes in the PVK HOMO level. Alternatively, if the light is absorbed directly from CdS, the charge transfer is in the opposite direction (holes from the VB of CdS to the HOMO of PVK). The surface passivation of the CdS QDs by surface ligands contributes to limit the interfacial charge transfer between the QDs and the polymer [3]. In our case the surface passivation by the residual thiol chains could be not as efficient as dodecanthiol since the chain length is reduced respect to the original cadmium-bis thiolate precursor upon the annealing treatment. Consequently the charge transfer effect on the photoluminescence quenching might be less effective. As third alternative, exciton (energy) transfer from PVK (band gap=3.6 eV) to CdS (band gap=3.08 eV from Table 1) followed by hole transfer back to PVK [3] could be in principle also possible due to good spectral overlap between the nanoparticles absorption and PVK emission. Nevertheless the energy transfer is unlikely to occur due to the fact that the distance among the QDs is much larger than the Förster radius. On the other hand the conductivity increase (Fig. 5) suggests that the QDs injects a non negligible density of holes and electrons in the polymer. Polarons created from injected electrons can quench the PVK photoluminescence very efficiently by excitation transfer.

4. Conclusions

The present study describes a simple one pot synthetic route for preparing CdS QDs through thermolysis of metal bis-thiolates in a high boiling solvent. Among the synthesis parameters, we found that a faster annealing process favors the formation of CdS QDs with narrow size distribution and good optical properties. After the synthesis, the QDs were dispersed in a PVK solution and a PVK:CdS nanocomposite was prepared at a 4% w/w ratio. The nanocomposite has been used to prepare a hybrid ITO/PVK:CdS/Al device that has shown two order of magnitude improved electrical conductivity respect to the ITO/PVK/Al reference device. In addition, a marked photoluminescence quenching has been observed as effect of the conductivity increase.

Acknowledgments

We thank Dr. A.M. Laera from ENEA Centro Ricerche Brindisi for providing the Cd precursor, Prof. M. De Crescenzi and Dr. S. Del Gobbo from Università degli Studi di Roma "Tor Vergata" for fruitful discussions.

Appendix A. Supporting information

Supplementary data associated with this article can be found in the online version at doi:10.1016/j.physe.2012.01.026.

References

[1] C.B. Murray, D.J. Norris, M.G. Bawendi, Journal of the American Chemical Society 115 (1993) 8706.
[2] (a) L.E. Brus, M. Nirmal, Accounts of Chemical Research 32 (1999) 407;
(b) D.J. Norris, M.G. Bawendi, L.E. Brus, Optical properties of semiconductor nanocrystals (quantum dots), in: J. Jortner, M. Ratner (Eds.), Molecular Electronics, Blackwell, Oxford, 1997, pp. 281–323;
(c) A.P. Alivisatos, Science 271 (1996) 933.
[3] A.P. Alivisatos, Journal of Physical Chemistry 100 (1996) 13226.
[4] (a) V.L. Colvin, M.C. Schlamp, A.P. Alivisatos, Nature 370 (1994) 354;
(b) M.V. Artemyev, V. Sperling, U.J. Woggon, Journal of Applied Physics 81 (10) (1997) 6975;
(c) J. Roither, W. Heiss, D.V. Talapin, N. Gaponik, A. Eychmuller, Applied Physics Letters 84 (2004) 2223.
[5] (a) A.G. Stanley, in: R. Wolfe (Ed.), Cadmium Sulfide Solar Cells, Applied Solid State Science, Academic Press, New York, 1975;
(b) A. Olea, P.J. Sebastian, Solar Energy Materials and Solar Cells 55 (1998) 149;
(c) G. Syrrokostas, M. Giannouli, P. Yianoulis, Renewable Energy 34 (2009) 1759;
(d) S. Krishnadasan, J. Tovilla, A.J. Vilar, A.J. deMello, J.C. deMello, Journal of Materials Chemistry 14 (2004) 2655.
[6] E. Chang, J.S. Miller, J.T. Sun, W.W. Yu, V.L. Colvin, R. Drezek, J.L. West, Biochemical and Biophysical Research Communications 334 (2005) 1317.
[7] (a) L.E. Brus, Journal of Chemical Physics 79 (1983) 5566;
(b) L.E. Brus, Journal of Chemical Physics 80 (1984) 4403.
[8] C. Petit, P. Lixon, M.P. Pileni, Journal of Physical Chemistry 94 (1990) 1598.
[9] (a) T. Vossmeyer, L. Katsikas, M. Giersig, I.G. Popovic, K. Diesner, A. Chemseddine, A. Eychmüller, H. Weller, Journal of Physical Chemistry 98 (1994) 7665;
(b) A.L. Rogach, A. Kornowski, M. Gao, A. Eychmüller, H. Weller, Journal of Physical Chemistry B 103 (1999) 3065;
(c) J.O. Winter, N. Gomez, S. Gatzert, C.E. Schmidt, B.A. Korgel, Colloids and Surfaces A 254 (2004) 147;
(d) T. Rajh, O.I. Mičić, A.J. Nozik, Journal of Physical Chemistry 97 (1993) 11999.
[10] (a) D.V. Talapin, A.L. Rogach, A. Kornowsky, M. Haase, H. Weller, Nano Letters 1 (4) (2001) 207;
(b) L. Manna, E.C. Scher, A.P. Alivisatos, Journal of the American Chemical Society 122 (2000) 12700;
(c) D. Yang, Q. Chen, S. Xu, Journal of Luminescence 126 (2) (2007) 853.
[11] (a) G. Carotenuto, B. Martorana, P. Perlo, L. Nicolais, Journal of Materials Chemistry 13 (2003) 2927;
(b) H. Tong, Y. Zhu, Nanotechnology 17 (2006) 845.
[12] F. Antolini, M. Pentimalli, T. Di Luccio, R. Terzi, M. Schioppa, M. Re, L. Mirenghi, L. Tapfer, Materials Letters 59 (2005) 3181.
[13] T. Di Luccio, A.M. Laera, L. Tapfer, S. Kempter, R. Kraus, B. Nickel, Journal of Physical Chemistry B 110 (2006) 12603.
[14] J. Ouyang, J. Kuijper, S. Brot, D. Kingston, X. Wu, D.M. Leek, M.Z. Hu, J.A. Ripmeester, K. Yu, Journal of Physical Chemistry C 113 (2009) 7579.

[15] F. Antolini, T. Di Luccio, M. Re, L. Tapfer, Crystal Research and Technology 40 (10–11) (2005) 948.
[16] C. Borriello, S. Masala, V. Bizzarro, G. Nenna, M. Re, E. Pesce, C. Minarini, T. Di Luccio, Journal of Applied Polymer Science 122 (2011) 3624.
[17] S. Masala, S. Del Gobbo, C. Borriello, V. Bizzarro, V. La Ferrara, M. Re, E. Pesce, C. Minarini, M. De Crescenzi, T. Di Luccio, Journal of Nanoparticle Research 13 (12) (2011) 6537. doi:10.1007/s11051-011-0558-x.
[18] Kyumin Lee, M. Duchamp, G. Kulik, A. Magrez, Jin Won Seo, S. Jeney, A.J. Kulik, L. Forró, Applied Physics Letters 91 (2007) 173112.
[19] Y. Wang, G. Meng, L. Zhang, C. Liang, J. Zhang, Chemistry of Materials 14 (2002) 1773.
[20] Scanning Probe Microscopy Training Notebook, Version 3, Digital Instruments/Veeco Metrology Group Inc., 2000.
[21] J.R. Sachleben, E.W. Wooten, L. Emsley, A. Pines, V.L. Colvin, A.P. Alivisatos, Chemical Physics Letters 198 (1992) 431.
[22] M.B. Khalifa, D. Vaufrey, A. Bouazizi, J. Tardy, H. Maaref, Materials Science and Engineering C 21 (2002) 277.
[23] A. Tang, F. Teng, L. Qian, Y. Hou, Y. Wang, Applied Physics Letters 95 (2009) 143115.
[24] S. Wang, S. Yang, C. Yang, Z. Li, J. Wang, W. Ge, Journal of Physical Chemistry B 104 (2000) 11853.
[25] (a) K.R. Choudhury, J.G. Winiarz, M. Samoc, P.N. Prasad, Applied Physics Letters 82 (3) (2003) 406;
(b) K.R. Choudhury, M. Samoc, A. Patra, P.N. Prasad, Journal of Physical Chemistry B 108 (2004) 1556.

Please cite this article as: S. Masala, et al., Physica E (2012), doi:10.1016/j.physe.2012.01.026